


THIRD PARTY BOREHOLE SEISMIC EXPERIMENTS DURING THE OCEAN DRILLING PROGRAM



1. Introduction

A 3D block diagram illustrating seismic wave propagation. The vertical axis on the left is labeled 'DEPTH KM' with a scale from 0 to 13. The horizontal axis at the top left is labeled 'VELOCITY KM/SEC.' with a scale from 0 to 8. The diagram shows four distinct layers: 'WATER' (0-2 km), 'SEDIMENT' (2-4 km), 'LAYER 2' (4-10 km), and 'LAYER 3' (10-13 km). Below 'LAYER 3' is the 'MANTLE'. A seismic wave source is shown on the surface, with concentric circles representing wave fronts. A ray path is traced from the source, showing a P-wave that travels through the layers, reflecting off the boundaries between LAYER 2 and LAYER 3, and between LAYER 3 and the MANTLE. The ray path is labeled with numbers 1 through 8, corresponding to the velocity scale.

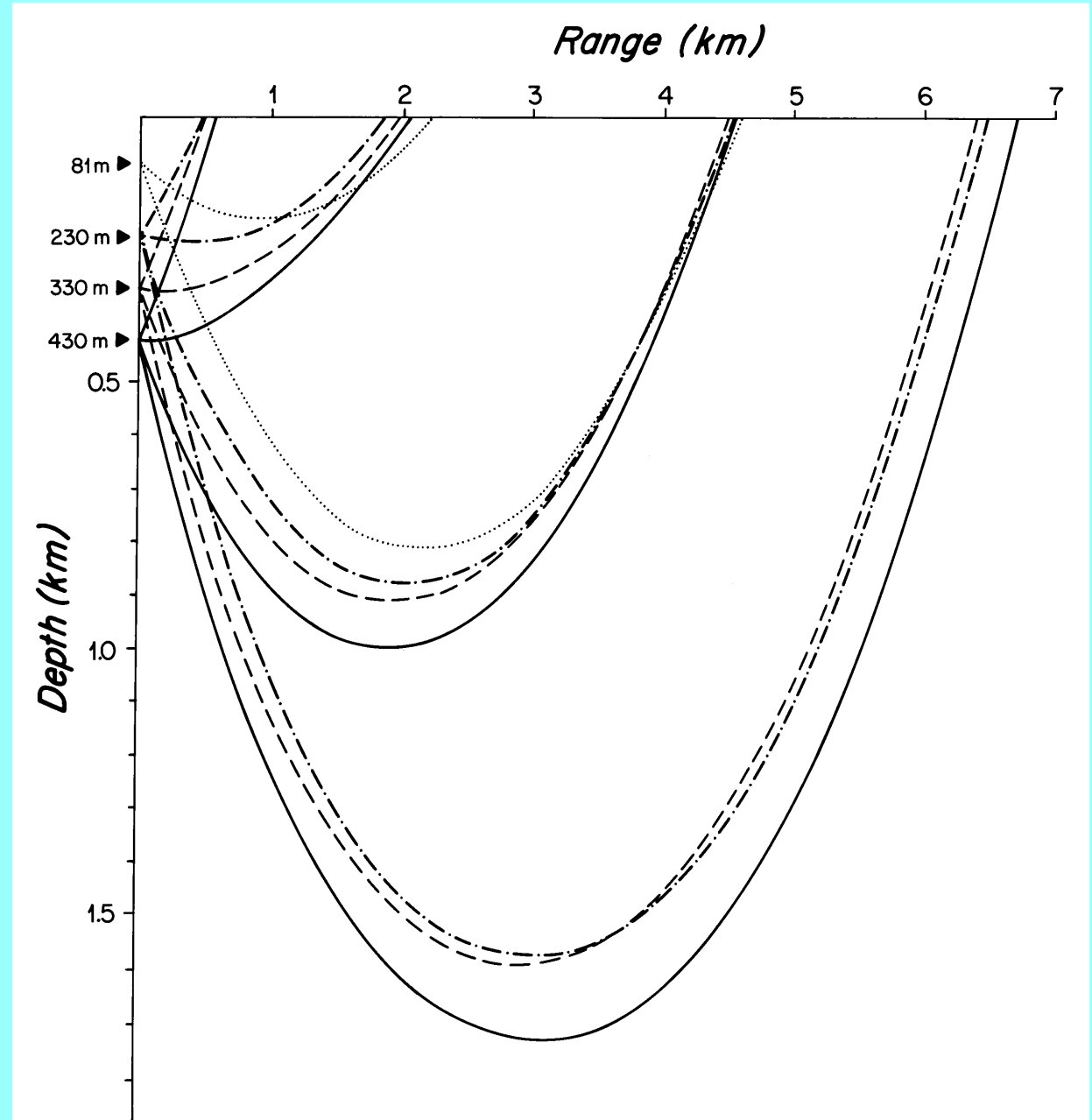


Figure 4: The first borehole seismic experiments on ODP were carried out at Sites 417 and 418 on Leg 102. [Swift and Stephen, 1989]



Figure 5: Raw (a) and filtered (b) data from the vertical channel at receiver depth 230m for the 4km airgun circle shot using ODP Leg 102. High frequency noise seen in the raw data (a) is most likely due to pipe banging in the borehole, the drill ship manuevering during recording intervals, and/or debris falling down the borehole. Bandpass filtered data (b) have been processed using a Butterworth filter at 2 and 20Hz. [Dougherty et al., 1995]

Figure 6: The coda after the principal P and S waves is caused by scattering from roughness and heterogeneity near the seafloor. Vertical channel data are compared for receivers at 230, 330, and 430m below the seafloor at azimuths parallel (a) and perpendicular (b) to the spreading direction. A summary of the Azimuthal dependence of the coda amplitude is given in Figure 7. [Dougherty et al., 1995]

Normal incidence VSP's [Balch and Lee, 1984] were carried out on ODP Legs 104, 109 and 111 [Leg 88 Shipboard Scientific Party, 1987b; Leg 109 Shipboard Scientific Party, 1988] before the VSP at Hole 735B on Leg 118 on the Southwest Indian Ridge. This experiment measured velocities corresponding to Layer 3 which was consistent with the gabbroic petrology of the cores. Anomalous high attenuation was also observed which prompted the hypothesis that the gabbro core may not actually represent the bulk of Layer 3 material (Figures 8 to 10).

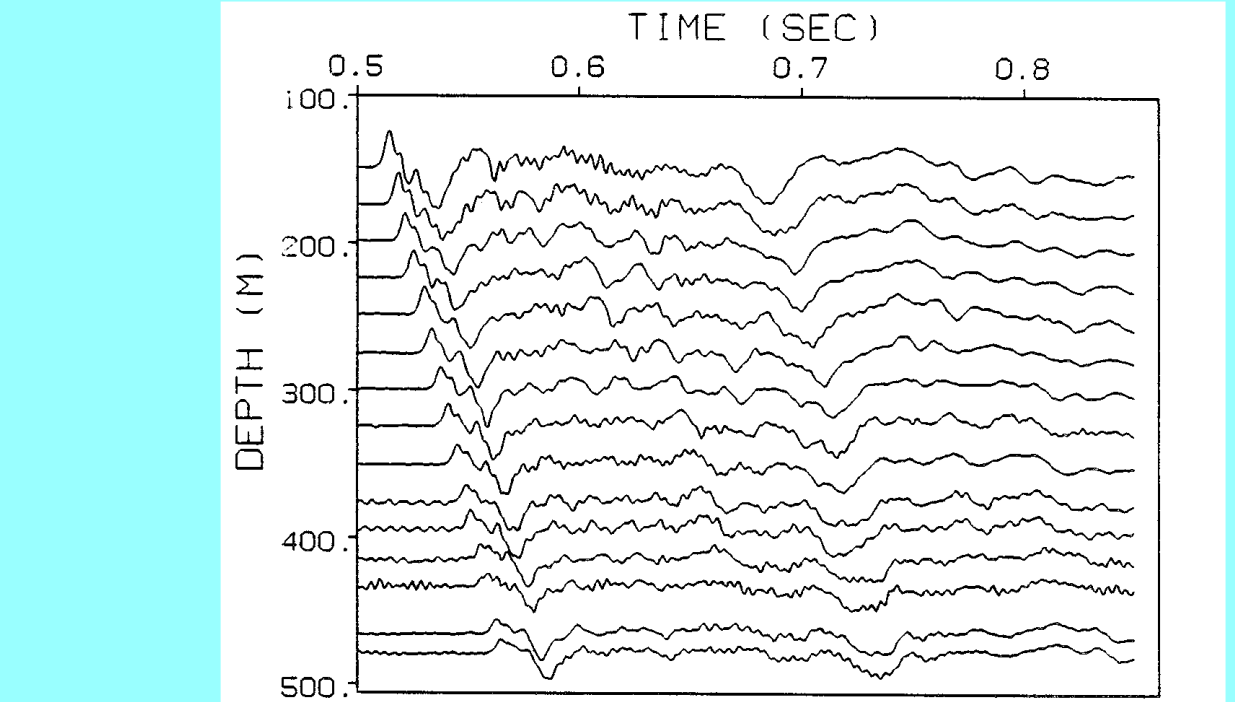


Figure 8: VSP seismograms cored at Holo 735B using a 1000 cubic inch airgun and a vertical component geophone. Depths in the borehole are given in meters below the seafloor; no sediments were found at Site 735. The seismograms were filtered to pass energy less than 250Hz; signal-to-noise ratios are 5-15dB in the 5-90Hz band. The small, upward deflection at 25m depth is probably an artifact of the airgun reflection, possibly from the null of the drilling ship. The data have been corrected for gain changes and spherical attenuation, so the decay in amplitude with borehole depth is due solely to attenuation. The loss of high frequency energy in the initial 50m over just 350s (less than a wavelength at 10Hz) can clearly be seen. [Swift et al., 1991; Swift and Stephen, 1992]

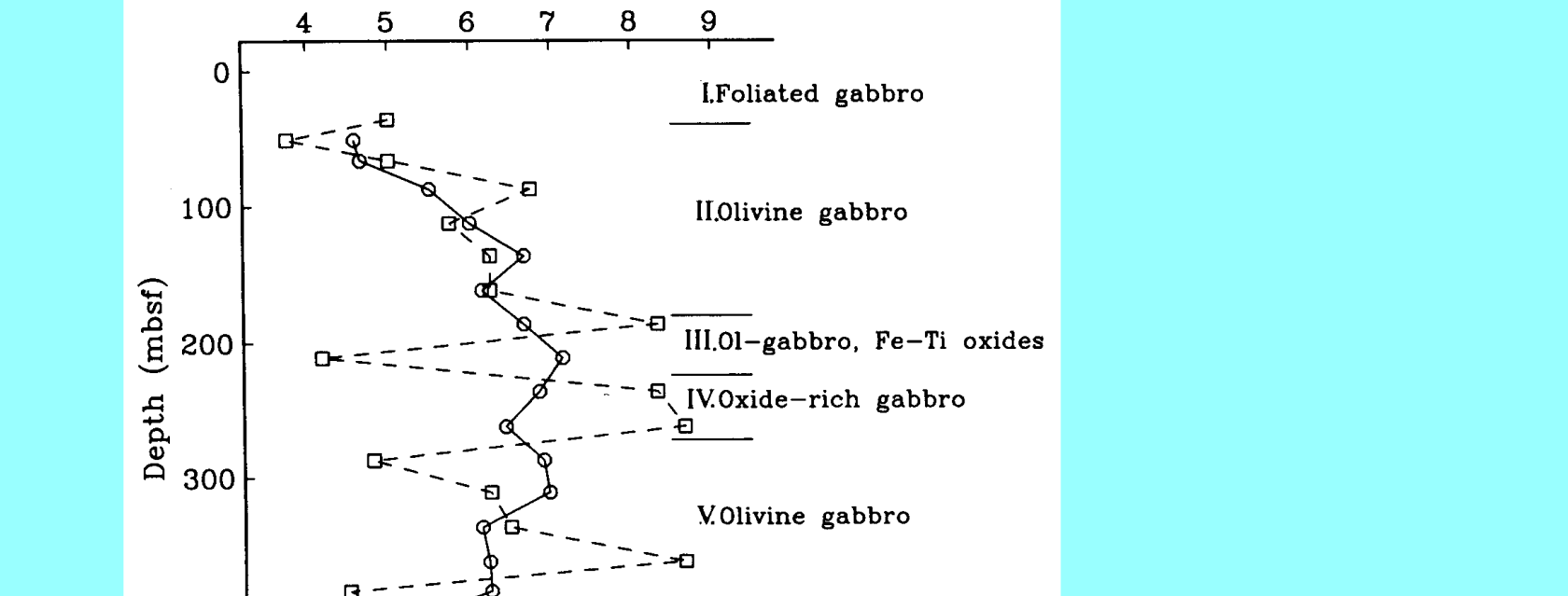


Figure 9: Interval velocities from one-way traveltimes to VSP receiver depths [Leg 118 Shipboard Scientific Party, 1989]. The dashed line connecting the squares represents raw data. The circles are solutions and subjective errors in the selection of seismic arrivals. The solid line connecting the circles indicates velocities after smoothing by a five-point moving average and is a more reliable velocity of the interval. The numbers and annotations are the lithologic units drilled, obtained at 1998ms. The travel time to them is truncated at a length in amplitude of the 19ms. (a) Spectral ratio, (b) amplitude ratios, (c) the amplitude ratios the slope of the amplitude ratios. The regression ratio corresponding to a Q_p of 1.0 is indicated.

Both offset and normal incidence VSPs were run on Leg 164 to study the seismic velocity structure of gas hydrates on the Blake Ridge, offshore South Carolina (Figure 13 and 14). Seismic velocities measured in three drill holes through the gas hydrate deposit indicate that substantial free gas exists at least 150 meters beneath the bottom-simulating reflector (BSR) (Figure 15). Both methane hydrate and free gas exist even where a clear BSR is absent. The low reflectance, or blanking, above the BSR is caused by lithologic homogeneity of the sediments rather than by hydrate cementation. (Holbrook et al., 1986; Leg 164 Shipboard Scientific Party, 1986; Leg 164 Shipboard Scientific Party, 1986b; Leg 164 Shipboard Scientific Party, 1986c; Leg 164 Shipboard Scientific Party, 1986d)

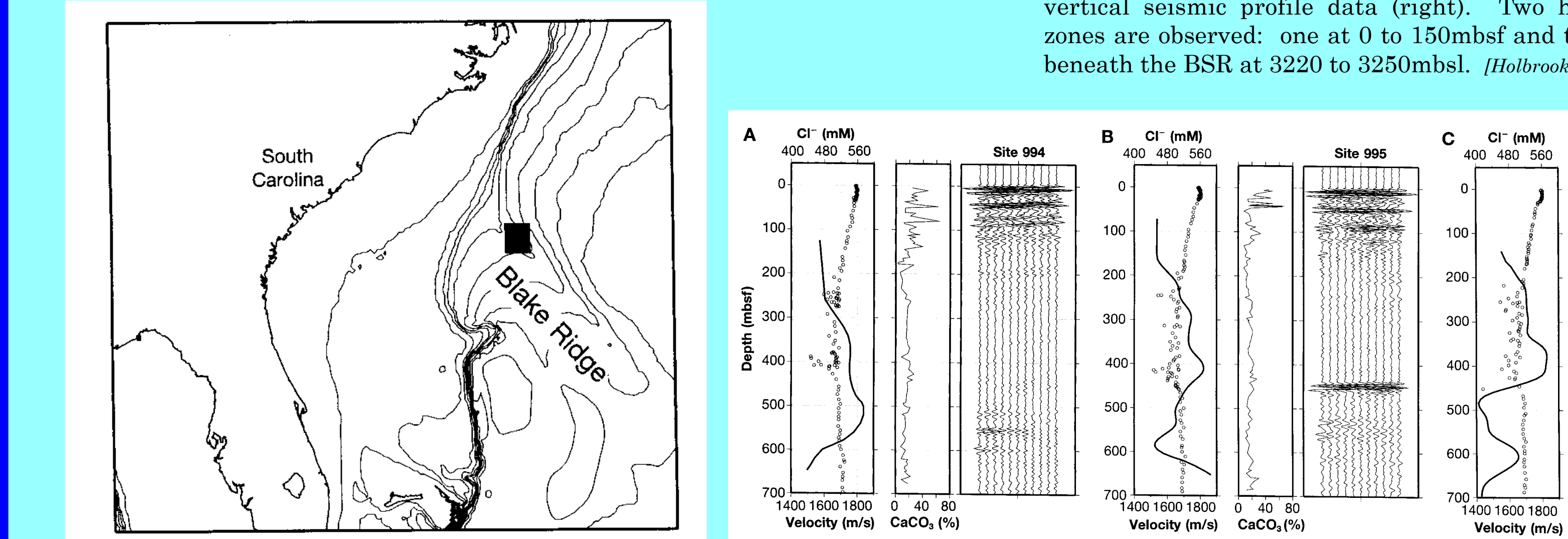
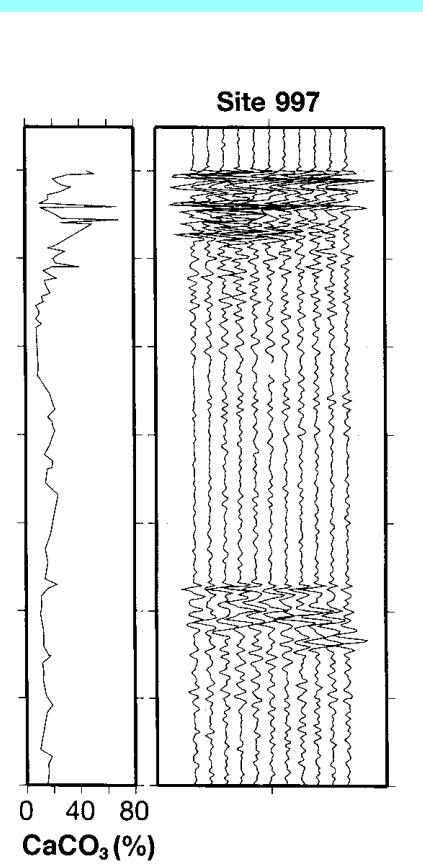


Figure 15: The seismic velocities from VSP's, the chlorinity, and the C_{org} compared with the vertical-incidence seismic reflection data from (A) Site 1002, (B) Site 1003, (C) Site 1004, (D) Site 1005, (E) Site 1006, (F) Site 1007, (G) Site 1008, (H) Site 1009, (I) Site 1010, (J) Site 1011, (K) Site 1012, (L) Site 1013, (M) Site 1014, (N) Site 1015, (O) Site 1016, (P) Site 1017, (Q) Site 1018, (R) Site 1019, (S) Site 1020, (T) Site 1021, (U) Site 1022, (V) Site 1023, (W) Site 1024, (X) Site 1025, (Y) Site 1026, (Z) Site 1027, (AA) Site 1028, (AB) Site 1029, (AC) Site 1030, (AD) Site 1031, (AE) Site 1032, (AF) Site 1033, (AG) Site 1034, (AH) Site 1035, (AI) Site 1036, (AJ) Site 1037, (AK) Site 1038, (AL) Site 1039, (AM) Site 1040, (AN) Site 1041, (AO) Site 1042, (AP) Site 1043, (AQ) Site 1044, (AR) Site 1045, (AS) Site 1046, (AT) Site 1047, (AU) Site 1048, (AV) Site 1049, (AW) Site 1050, (AX) Site 1051, (AY) Site 1052, (AZ) Site 1053, (BA) Site 1054, (BB) Site 1055, (BC) Site 1056, (BD) Site 1057, (BE) Site 1058, (BF) Site 1059, (BG) Site 1060, (BH) Site 1061, (BI) Site 1062, (BJ) Site 1063, (BK) Site 1064, (BL) Site 1065, (BM) Site 1066, (BN) Site 1067, (BO) Site 1068, (BP) Site 1069, (BQ) Site 1070, (BR) Site 1071, (BS) Site 1072, (BT) Site 1073, (BU) Site 1074, (BV) Site 1075, (BW) Site 1076, (BX) Site 1077, (BY) Site 1078, (BZ) Site 1079, (CA) Site 1080, (CB) Site 1081, (CC) Site 1082, (CD) Site 1083, (CE) Site 1084, (CF) Site 1085, (CG) Site 1086, (CH) Site 1087, (CI) Site 1088, (CJ) Site 1089, (CK) Site 1090, (CL) Site 1091, (CM) Site 1092, (CN) Site 1093, (CO) Site 1094, (CP) Site 1095, (CQ) Site 1096, (CR) Site 1097, (CS) Site 1098, (CT) Site 1099, (CU) Site 1100, (CV) Site 1101, (CW) Site 1102, (CX) Site 1103, (CY) Site 1104, (CZ) Site 1105, (DA) Site 1106, (DB) Site 1107, (DC) Site 1108, (DD) Site 1109, (DE) Site 1110, (DF) Site 1111, (DG) Site 1112, (DH) Site 1113, (DI) Site 1114, (DJ) Site 1115, (DK) Site 1116, (DL) Site 1117, (DM) Site 1118, (DN) Site 1119, (DO) Site 1120, (DP) Site 1121, (DQ) Site 1122, (DR) Site 1123, (DS) Site 1124, (DT) Site 1125, (DU) Site 1126, (DV) Site 1127, (DW) Site 1128, (DX) Site 1129, (DY) Site 1130, (DZ) Site 1131, (EA) Site 1132, (EB) Site 1133, (EC) Site 1134, (ED) Site 1135, (EE) Site 1136, (EF) Site 1137, (EG) Site 1138, (EH) Site 1139, (EI) Site 1140, (EJ) Site 1141, (EK) Site 1142, (EL) Site 1143, (EM) Site 1144, (EN) Site 1145, (EO) Site 1146, (EP) Site 1147, (EQ) Site 1148, (ER) Site 1149, (ES) Site 1150, (ET) Site 1151, (EU) Site 1152, (EV) Site 1153, (EW) Site 1154, (EX) Site 1155, (EY) Site 1156, (EZ) Site 1157, (FA) Site 1158, (FB) Site 1159, (FC) Site 1160, (FD) Site 1161, (FE) Site 1162, (FF) Site 1163, (FG) Site 1164, (FH) Site 1165, (FI) Site 1166, (FJ) Site 1167, (FK) Site 1168, (FL) Site 1169, (FM) Site 1170, (FN) Site 1171, (FO) Site 1172, (FP) Site 1173, (FQ) Site 1174, (FR) Site 1175, (FS) Site 1176, (FT) Site 1177, (FU) Site 1178, (FV) Site 1179, (FW) Site 1180, (FX) Site 1181, (FY) Site 1182, (FZ) Site 1183, (GA) Site 1184, (GB) Site 1185, (GC) Site 1186, (GD) Site 1187, (GE) Site 1188, (GF) Site 1189, (GG) Site 1190, (GH) Site 1191, (GI) Site 1192, (GJ) Site 1193, (GK) Site 1194, (GL) Site 1195, (GM) Site 1196, (GN) Site 1197, (GO) Site 1198, (GP) Site 1199, (GQ) Site 1200, (GR) Site 1201, (GS) Site 1202, (GT) Site 1203, (GU) Site 1204, (GV) Site 1205, (GW) Site 1206, (GX) Site 1207, (GY) Site 1208, (GZ) Site 1209, (HA) Site 1210, (HB) Site 1211, (HC) Site 1212, (HD) Site 1213, (HE) Site 1214, (HF) Site 1215, (HG) Site 1216, (HH) Site 1217, (HI) Site 1218, (HJ) Site 1219, (HK) Site 1220, (HL) Site 1221, (HM) Site 1222, (HN) Site 1223, (HO) Site 1224, (HP) Site 1225, (HQ) Site 1226, (HR) Site 1227, (HS) Site 1228, (HT) Site 1229, (HU) Site 1230, (HV) Site 1231, (HW) Site 1232, (HX) Site 1233, (HY) Site 1234, (HZ) Site 1235, (IA) Site 1236, (IB) Site 1237, (IC) Site 1238, (ID) Site 1239, (IE) Site 1240, (IF) Site 1241, (IG) Site 1242, (IH) Site 1243, (II) Site 1244, (IJ) Site 1245, (IK) Site 1246, (IL) Site 1247, (IM) Site 1248, (IN) Site 1249, (IO) Site 1250, (IP) Site 1251, (IQ) Site 1252, (IR) Site 1253, (IS) Site 1254, (IT) Site 1255, (IU) Site 1256, (IV) Site 1257, (IW) Site 1258, (IX) Site 1259, (IY) Site 1260, (IZ) Site 1261, (JA) Site 1262, (JB) Site 1263, (JC) Site 1264, (JD) Site 1265, (JE) Site 1266, (JF) Site 1267, (JG) Site 1268, (JH) Site 1269, (JI) Site 1270, (JJ) Site 1271, (JK) Site 1272, (JL) Site 1273, (JM) Site 1274, (JN) Site 1275, (JO) Site 1276, (JP) Site 1277, (JQ) Site 1278, (JR) Site 1279, (JS) Site 1280, (JT) Site 1281, (JU) Site 1282, (JV) Site 1283, (JW) Site 1284, (JX) Site 1285, (JY) Site 1286, (JZ) Site 1287, (KA) Site 1288, (KB) Site 1289, (KC) Site 1290, (KD) Site 1291, (KE) Site 1292, (KF) Site 1293, (KG) Site 1294, (KH) Site 1295, (KI) Site 1296, (KJ) Site 1297, (KK) Site 1298, (KL) Site 1299, (KM) Site 1300, (KN) Site 1301, (KO) Site 1302, (KP) Site 1303, (KQ) Site 1304, (KR) Site 1305, (KS) Site 1306, (KT) Site 1307, (KU) Site 1308, (KV) Site 1309, (KW) Site 1310, (KX) Site 1311, (KY) Site 1312, (KZ) Site 1313, (LA) Site 1314, (LB) Site 1315, (LC) Site 1316, (LD) Site 1317, (LE) Site 1318, (LF) Site 1319, (LG) Site 1320, (LH) Site 1321, (LI) Site 1322, (LJ) Site 1323, (LK) Site 1324, (LL) Site 1325, (LM) Site 1326, (LN) Site 1327, (LO) Site 1328, (LP) Site 1329, (LQ) Site 1330, (LR) Site 1331, (LS) Site 1332, (LT) Site 1333, (LU) Site 1334, (LV) Site 1335, (LW) Site 1336, (LX) Site 1337, (LY) Site 1338, (LZ) Site 1339, (MA) Site 1340, (MB) Site 1341, (MC) Site 1342, (MD) Site 1343, (ME) Site 1344, (MF) Site 1345, (MG) Site 1346, (MH) Site 1347, (MI) Site 1348, (MJ) Site 1349, (MK) Site 1350, (ML) Site 1351, (MM) Site 1352, (MN) Site 1353, (MO) Site 1354, (MP) Site 1355, (MQ) Site 1356, (MR) Site 1357, (MS) Site 1358, (MT) Site 1359, (MU) Site 1360, (MV) Site 1361, (MW) Site 1362, (MX) Site 1363, (MY) Site 1364, (MZ) Site 1365, (NA) Site 1366, (NB) Site 1367, (NC) Site 1368, (ND) Site 1369, (NE) Site 1370, (NF) Site 1371, (NG) Site 1372, (NH) Site 1373, (NI) Site 1374, (NJ) Site 1375, (NK) Site 1376, (NL) Site 1377, (NM) Site 1378, (NN) Site 1379, (NO) Site 1380, (NP) Site 1381, (NQ) Site 1382, (NR) Site 1383, (NS) Site 1384, (NT) Site 1385, (NU) Site 1386, (NV) Site 1387, (NW) Site 1388, (NX) Site 1389, (NY) Site 1390, (NZ) Site 1391, (OA) Site 1392, (OB) Site 1393, (OC) Site 1394, (OD) Site 1395, (OE) Site 1396, (OF) Site 1397, (OG) Site 1398, (OH) Site 1399, (OI) Site 1400, (OJ) Site 1401, (OK) Site 1402, (OL)



CaCO₃ content are 1994, (B) Site 995 hydrate is present plate with vertical is indicative of free e above the BSR is [6]

The ODP core also saw redevelopment of systems for re-entering boreholes from conventional research vessels (Figure 16) and submersibles after the drill ship left the site (Igarashi *et al.*, 1988; Montagner *et al.*, 1989a; *et al.*, 1992). Borehole seismic experiments and installations that used this wireline re-entry technique were carried out in SDSP Holes 534 (Blake-Bahama Basin) (Bradley *et al.*, 1997; Stephen *et al.*, 1994) and 396 (Mid-Atlantic Ridge at 23degrees north) (Montagner *et al.*, 1989a) and ODP Hole 843B (south of Oahu [Collins *et al.*, 2001; Dziekonski *et al.*, 1992; Stephen *et al.*, 2003; Sutherland *et al.*, submitted]). The latter experiment (the Ocean Seismic Network Pilot Experiment) carried out a test of three configurations of broadband shallow seismic installation in preparation for extending the Global Seismic Network to the deep ocean.

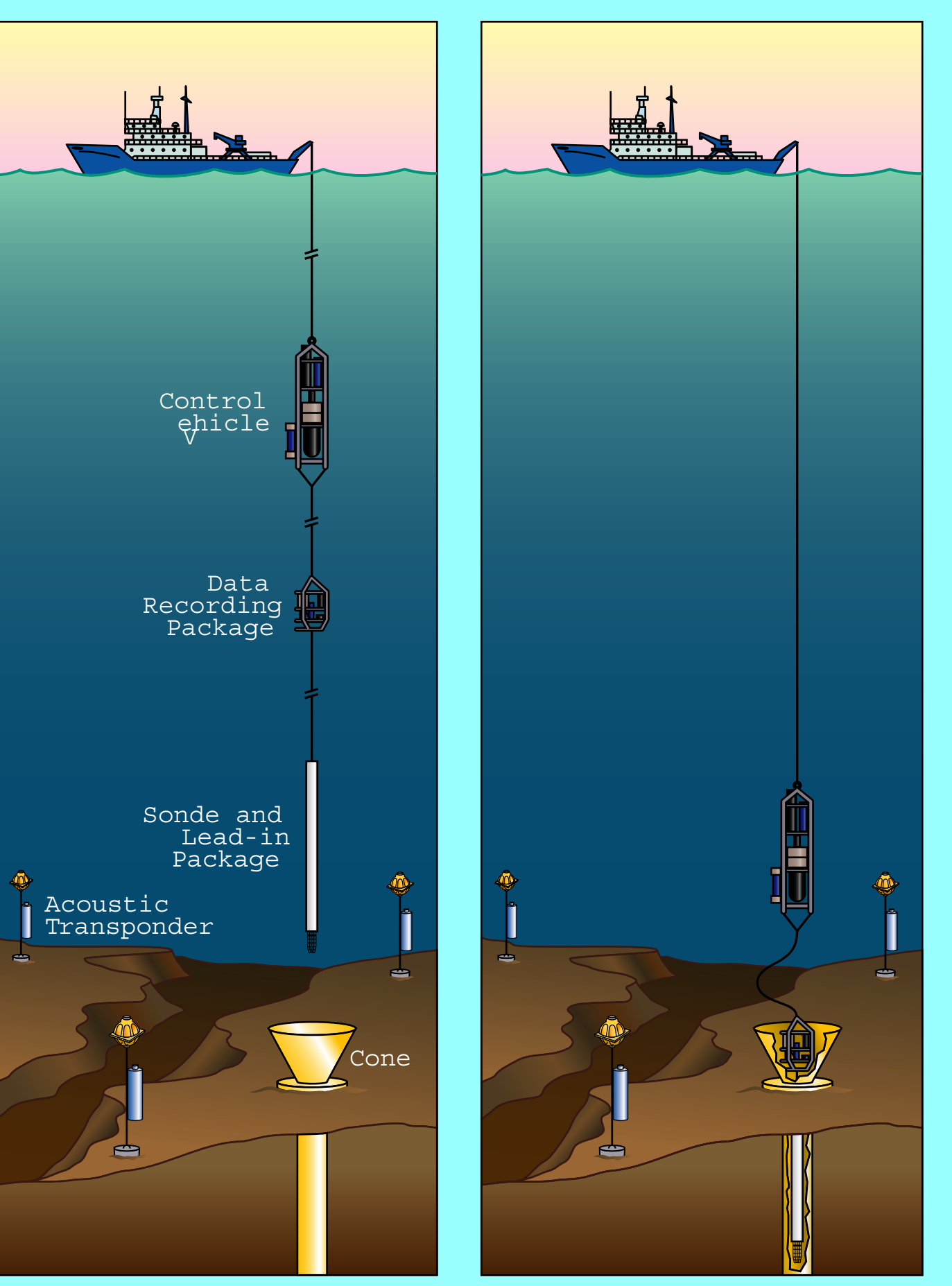


Figure 16: In the Wireline Re-entry System a borehole sonde, data recording package and control vehicle are suspended from a conventional research vessel on co-axial or fibre-optic cable (left). The control vehicle, navigated within a network of acoustic transponders, is used to guide the sonde into the borehole. The sonde is lowered into the borehole until the data recording package lands in the re-entry cone (right). When the seafloor and subsurface systems are operating properly the control vehicle is disconnected from the data recording package and is recovered by a separate recovery ship. The borehole system acquires data autonomously for up to a year until the system is recovered by grappling. (*Spies et al., 1992*)

A new innovation on ODP was the deployment of broadband seismometers in boreholes. Whereas the conventional VSPs and offset VSPs mentioned above

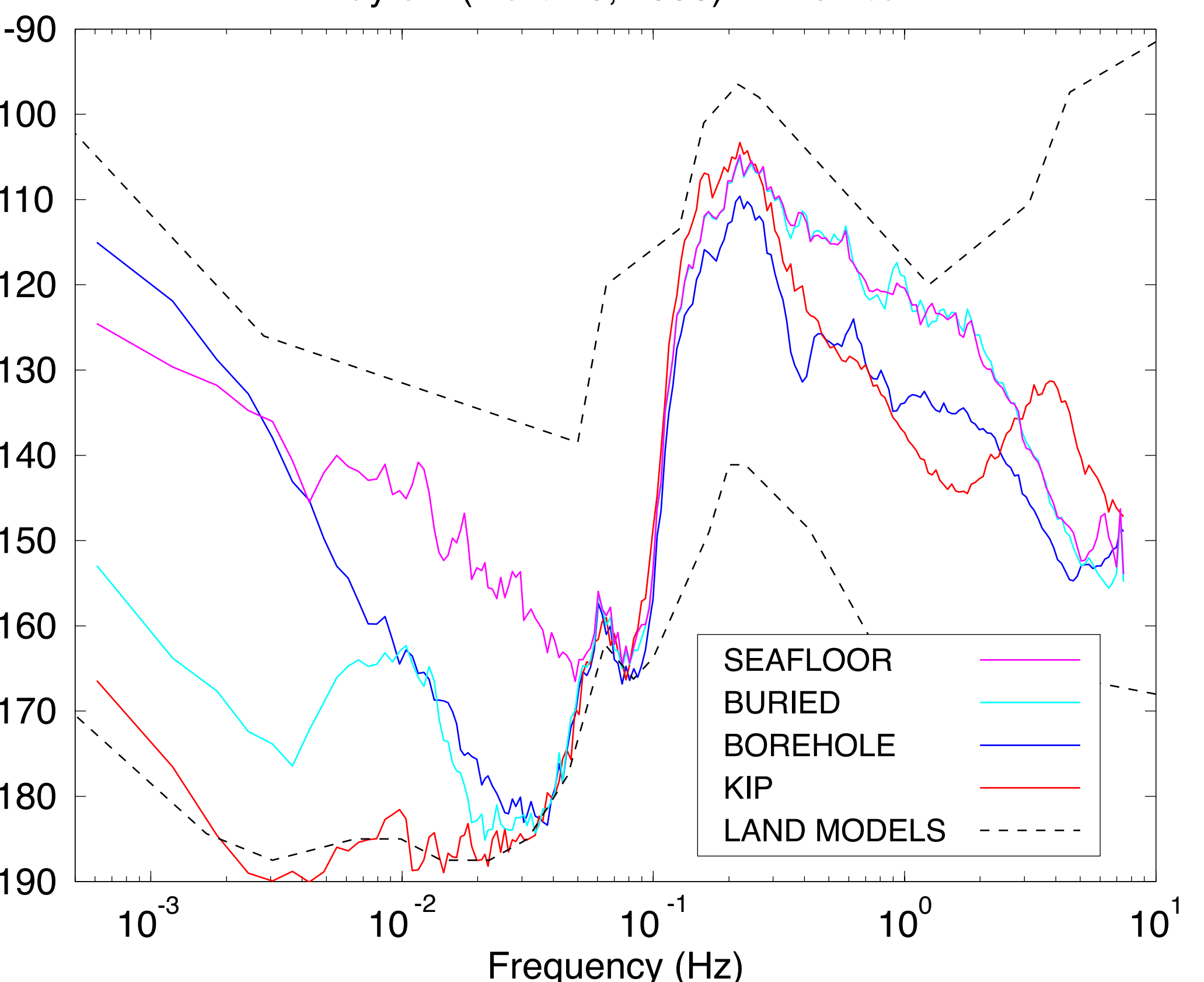


Figure 17: Vertical component spectra for the three broadband seismometer configurations deployed on the OSNPE (seafloor, buried and borehole) and the Kipapa GSN station on Oahu are compared with high and low noise spectral models based on land observations. From 20mHz to 100mHz the borehole and buried sensors in the ocean are as quiet as any land sensor.

air, R.G., M.M. Harris, J.A. Orcutt, and T.H. Jordan, Descriptive performance of the marine seismic system during the Njord-88 experiment, Initial Reports of the Deep Sea Drilling Project, 5

[illegible]

In thick sedimentary sequences VSP's can be very useful in correlating the drilling results with the seismic reflection profiling results. This was demonstrated on ODP Leg 123 which drilled in the Argo Abyssal Plain (Figure 11) (*Leg 123 Shipboard Scientific Party, 1990a*; *Leg 123 Shipboard Scientific Party, 1990b*). VSP's were also carried out on ODP Legs 127/128, 129, 131

Figure 7 consists of two polar plots, (a) and (b), showing coda energy as a function of azimuth and depth. Plot (a) is for a depth of 230m and plot (b) is for a depth of 430m. Both plots show energy contours with a color scale from 0 to 100. The azimuth ranges from 210° to 150°. Plot (a) shows a prominent energy peak around 180° azimuth, while plot (b) shows a more complex pattern with multiple peaks and troughs.

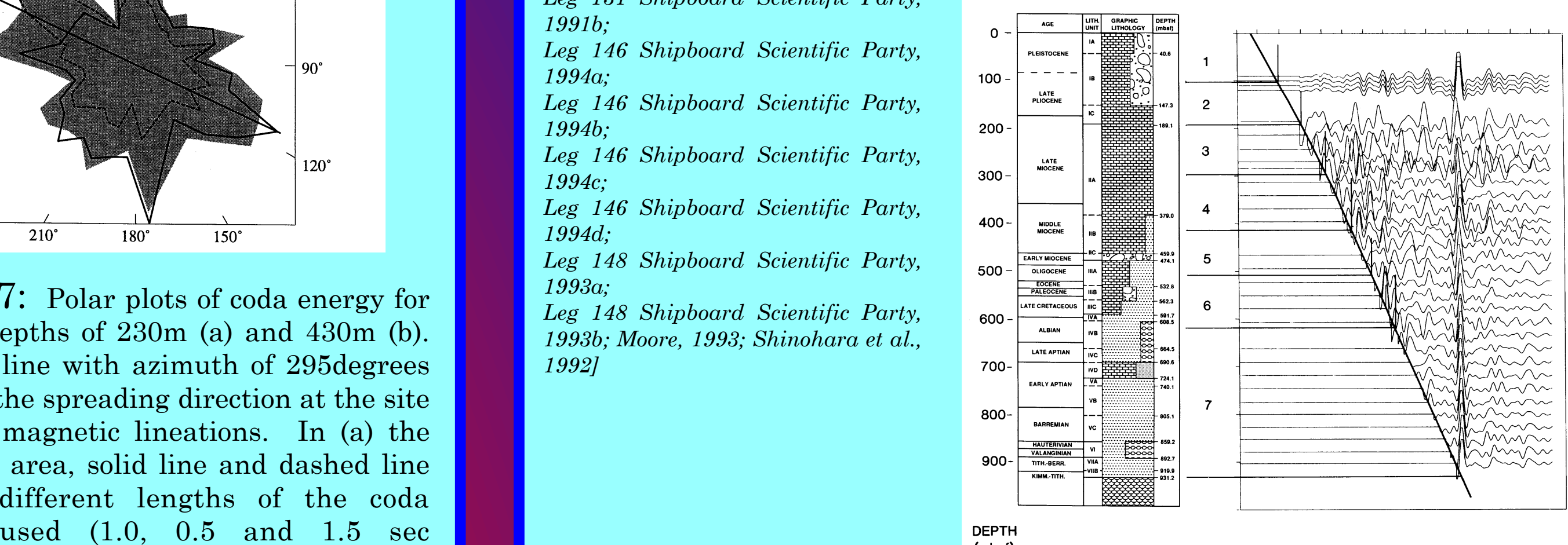


Figure 11: The Leg 123 VSP data was processed by separating the total field into separate upgoing and downgoing wavefields. This figure shows the upgoing wavefield for an airgun source. The processing involved separating all reflections into the sedimentary section between 8.25 and 8.5 s and a sub-basement reflector at 8.86sec. The traces between 0.9 and 150msbf are a stack of the deconvolved VSP data (traveltimes are two-way propagation). The VSP section can be used to correlate the BMR seismic reflection line (top) with the drilling results (left side). The seismic sequences are numbered. [Blmer et al., 1992]

The VSP data acquired at Hole 504B in the eastern equatorial Pacific on Leg 148 helped to constrain the velocity-depth structure at the site [Leg 109 Shipboard Scientific Party, 1988; Leg 148 Shipboard Scientific Party, 1993a; Leg 148 Shipboard Scientific Party, 1993b; Swift et al., 1996; Swift et al., 1998a; Swift et al., 1998b] and showed that upper Layer 3 at this site, at a depth of over 2 km into the crust, did not consist of gabbro but rather consisted of the lower portions of the sheeted dykes (Figure 12) [Detrick et al., 1993]. VSPs were also carried out on Leg 156 [Leg 156 Shipboard Scientific Party, 1995a; Leg 156 Shipboard Scientific Party, 1995b; Leg 156 Shipboard Scientific Party, 1995c].

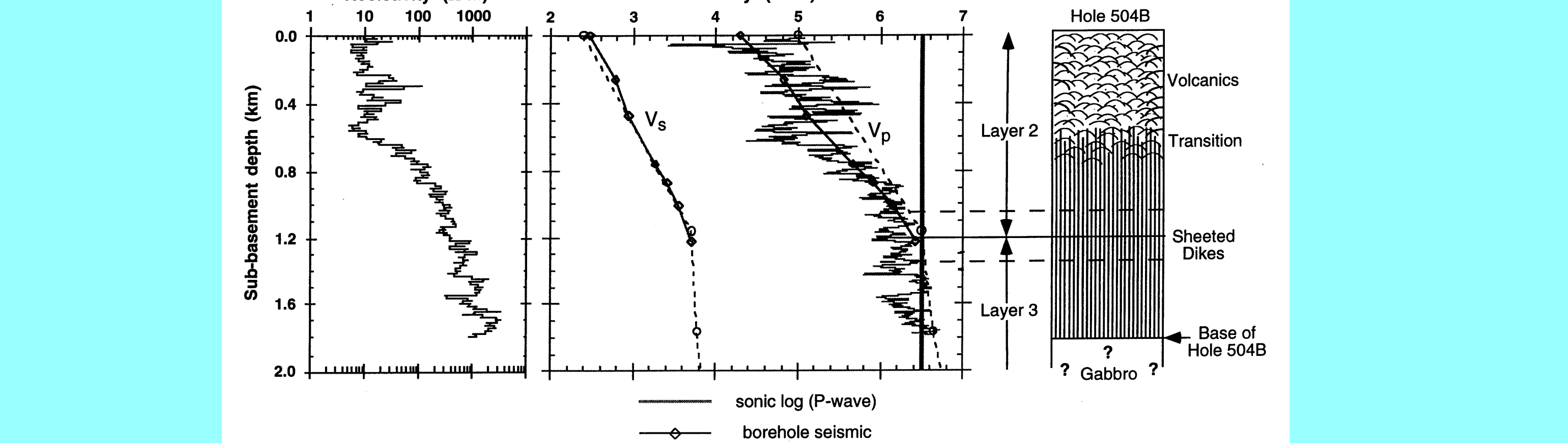


Figure 12: The variation in bulk resistivity downhole derived from logging in Hole 504B, the crustal velocity structure at the borehole and the lithostratigraphy. The crustal velocity model is based on a Layer 3 velocity of 6.5km/sac derived from sonobuoy studies and Hole 504B (vertical bar) and a linear regression of the shallow crustal velocity gradient determined from travel-time and amplitude modeling of the borehole seismic experiment (thick solid line). For comparison, the thin grey line shows the sonic velocity log and the dashed line shows the sonobuoy velocity model. The change in the vertical velocity gradient that defines the Layer 2/3 boundary at 1.2±0.2km sub-basement, occurs within the sheeted-de dyke section, about 660m above the base of the Layer 2. At least the upper 400-800m of seismic layer 3 consists of dolerites and metadolerites rather than gabbro. [Detrick et al., 1998]

[illegible]